Ab Initio Bonding, Molecular Structure, and Quadrupole Coupling Constants of Aluminum Chlorides

Gilbert J. Mains,[†] Evangelos A. Nantsis,[‡] and W. Robert Carper*,[§]

Department of Chemistry, Oklahoma State University, Stillwater, Oklahoma 74078, Department of Chemistry, Wichita State University, Wichita, Kansas 67260-0051, and Institut für Physikalische Chemie, RWTH Aachen, D-52056 Aachen, Germany

Received: December 20, 2000; In Final Form: February 16, 2001

The ab initio structures and energies of a series of gas-phase aluminum chlorides have been calculated at the RHF/6-31G* and MP2/6-31G* levels. The vibrational spectra of $AlCl_3$, Al_2Cl_6, $AlCl_4^-$, $EtAlCl_3^-$, $Al_2Cl_7^-$, $Et_2Al_2Cl_5^-$, and *trans*-$Et_2Al_2Cl_4$ are calculated at the RHF/6-31G* level. The theoretical vibrational spectra closely match the experimental (liquid state) infrared and Raman spectra and require a scale factor of 0.97 to yield a correlation coefficient (R^2) of 0.999. The ^{27}Al quadrupole coupling constants and asymmetry parameters of the electric field gradient tensor have been calculated for a series of aluminum compounds (Al_2Br_6, Al_2Cl_6, AlF, $Al_2(CH_3)_6$) at the HF/3-21G, B3LYP/6-31G*//HF/3-21G, HF/6-31G*//HF/3-21G, HF/6-31G*, B3LYP/6-31G*//HF/6-31G*, B3LYP/6-31G*, and B3LYP/cc-pVTZ levels. The correlation coefficient between experimental and theoretical ^{27}Al nuclear quadrupole coupling constants (NQCC) varies from 0.984 for the HF/3-21G calculation to 0.9986 for the density functional theory (DFT) B3LYP/cc-pVTZ result. The theoretical values of the ^{27}Al NQCC vary from −46.92 MHz (HF/3-21G) to −37.17 MHz (B3LYP/cc-pVTZ).

Introduction

Room-temperature chloroaluminate melts (ionic liquids) provide excellent model systems for spectroscopic studies, including vibrational and NMR spectrocopy.[1−14] Studies of the room-temperature chloroaluminate melts have identified various Al-containing species including $AlCl_4^-$ and $Al_2Cl_7^-$ in melts formed from $AlCl_3$ and organic chlorides.[1−7] Similar species such as $EtAlCl_3^-$ and $Et_2Al_2Cl_5^-$ have also been reported in melts containing dimeric ethylaluminum dichloride and organic chlorides.[8−11]

The successful use of both semiemprical (PM3) and ab initio theoretical models (gas phase) of melt components[12−14] has led to this ab initio study of Al-containing chloroaluminate melt species. In this study the results of ab initio calculations at the RHF/6-31G* level are compared with previously reported liquid-state vibrational spectra for $AlCl_4^-$, $EtAlCl_3^-$, $Al_2Cl_7^-$, $Et_2Al_2Cl_5^-$, and *trans*-$Et_2Al_2Cl_4$. Of particular interest is the small scaling factor (0.97) used when calculated and experimental vibrational spectra of these aluminum containing species are compared.

An important physical parameter that can also be determined by ab initio methods is the nuclear quadrupole coupling constant (NQCC) and its associated electric field gradients (EFG's). It has been shown that NQCC's can be obtained experimentally and provide information about the electronic structure of a molecule in its ground state. The NQCC's are important because they are sensitive to the shape of electronic charge distribution in molecules. Consequently, NQCC's can be used to provide quantitative estimates of hybridization, electronegativities, ionic character, bonding character, etc. NQCC's obtained from ab initio calculations involve the evaluation of the EFG's that are directly proportional to NQCC values. Electric field gradients (EFG's) determined theoretically are heavily dependent on the level (method) of computation, each of which provide a different numerical value for a given molecule.

In this investigation a correlation is established between experimental ^{27}Al NQCC's and their corresponding theoretical EFG's so that accurate NQCC's can be obtained by ab initio calculations for other ^{27}Al-containing species as well. This was accomplished by first obtaining experimental NQCC's values from the literature for ^{27}Al-containing molecules. The EFG's are calculated for these Al-containing molecules at computational levels including HF/3-21G, B3LYP/6-31G*//HF/3-21G, HF/6-31G*//HF/3-21G, HF/6-31G*, B3LYP/6-31G*//HF/6-31G*, B3LYP/6-31G*, and B3LYP/cc-pVTZ. The experimental NQCC's (χ_{ij}) are correlated with EFG's (q_{ij}) using eq 1:

$$\chi_{ij} = cq_{ij} \tag{1}$$

Each quantum mechanical method yields a slightly different proportionality coefficient constant c, so that regardless of the level of calculation, the same NQCC is obtained. This study also addresses how the use of fully optimized geometries from low-level calculations like HF/3-21G affect the correlation coefficient c when it is used for single point calculation at higher computational levels including HF/6-31G*//HF/3-21G and B3LYP/6-31G*//HF/3-21G.

Computational Methods

The GAUSSIAN 92 and GAUSSIAN 94 programs[15,16] were used for the ab initio vibrational frequency calculations. The GAUSSIAN 98 program[17] was used for the NQCC and EFG calculations. The structures were initially calculated with the semiempirical MOPAC6 program[18] and refined using ab initio methods. The vibrational frequencies were computed at the RHF/6-31G* level. The eigenvectors for each normal mode were

* Corresponding author. E-mail: carper@wsuhub.uc.twsu.edu.
[†] Oklahoma State University.
[‡] Wichita State University.
[§] Institut für Physikalische Chemie.

10.1021/jp004549w CCC: $20.00
Published on Web 04/04/2001

displayed on the computer and identified according to which molecular motions dominated. Electron correlation for all of the structures was partially included by performing Moeller–Plesset perturbation[19] calculations at the MP2/6-31G* level.

Nuclear Quadrupole Coupling Constants. After the geometry optimization the EFG tensor is evaluated by using the PRISM algorithm. The values $\mathbf{V}_{zz}$, $\mathbf{V}_{xx}$, $\mathbf{V}_{yy}$ of the EFG tensor are used to calculate χ and the asymmetry parameter, η. These calculations are detailed in the theory section that follows. The experimental NQCC's are plotted against the calculated EFG's. One uses a least-squares fit between c_{ii} and q_{ii} while forcing the intercept to go through the origin (the intercept has to be zero because molecules with a spherical charge distribution will yield a NQCC equal to zero) and obtains a slope. The NQCC (in millibarns) is calculated from the slope. The relationship between the NQCC and EFG's is c_{ii} (MHz) $= -0.234965Q$ (mb) $\times$ q_{ii} (au).

Theory. Quadrupolar nuclei ($I \geq 1$) are associated with a parameter known as the nuclear quadrupolar coupling constant (χ_{zz} in MHz). χ_{zz} is a second rank tensor and is related to the electric field gradient, EFG ($\mathbf{V}_{ij}$) by

$$\chi_{ij} = e^2 Q \mathbf{V}_{ij}/h \tag{2}$$

where e is the unit of electrostatic charge, h is Planck's constant, and Q is the quadrupole moment, which is a constant depending on the nucleus. The EFG is defined by a 3×3 symmetric tensor,

$$\mathbf{V}_{ij} = \partial^2\mathbf{V}/\partial\mathbf{x}^2, \partial\mathbf{y}^2, \partial\mathbf{z}^2 \tag{3}$$

where $\mathbf{V}$ is the electrostatic potential at nucleus due to the surrounding charges.

The EFG can be expressed in an axis system so that it is diagonalized and produces a traceless tensor, called the principal axis system of the electric field gradient tensor.

$$\partial^2\mathbf{V}/\partial\mathbf{x}^2 + \partial^2\mathbf{V}/\partial\mathbf{y}^2 + \partial^2\mathbf{V}/\partial\mathbf{z}^2 \quad \text{or} \quad \mathbf{V}_{xx} + \mathbf{V}_{yy} + \mathbf{V}_{zz} = 0 \tag{4}$$

By convention, the EFG tensor is expressed in terms of two quantities,

$$\mathbf{eq}_{zz} = \mathbf{V}_{zz} = \partial^2\mathbf{V}/\partial\mathbf{z}^2 \quad \text{and} \quad \eta = (\mathbf{V}_{xx} - \mathbf{V}_{yy})/\mathbf{V}_{zz} \tag{5}$$

The second parameter η is called the asymmetry parameter and measures the deviation of the field gradient tensor from axial symmetry. Also by convention $|\mathbf{V}_{zz}| \geq |\mathbf{V}_{yy}| \geq |\mathbf{V}_{xx}|$ so that η ranges from 0 to 1.[20–29]

The EFG tensor at the nucleus I has the form

$$\mathbf{eq}(\mathrm{I}) = \mathbf{e}[\Sigma_{k=I}\mathbf{Z}_k(3\mathbf{R}_{Ik}\mathbf{R}_{Ik} - \mathbf{R}^2_{Ik}\,1)/\mathbf{R}^j_{Ik} - \langle\Psi|\Sigma(3\mathbf{r}_{Ij}\mathbf{r}_{Ij} - \mathbf{r}_{Ij}^2\,1)/r^j_{Ij}|\Psi\rangle \tag{6}$$

where $\mathbf{Z}_k$ is the charge of nucleus k, $\mathbf{R}_{Ik}$ is a vector from nucleus I to k, 1 is a unit dyadic, ψ is the electronic wave function of a molecule in the ground state and $\mathbf{r}_{Ij}$ is a vector from nucleus I to electron j.

The first term in eq 6 represents the nuclear contribution, and the second term represents the electronic contribution to the EFG tensor at the nucleus I. The nuclear coterm can be estimated in terms of a classical approach; however, the electronic term in the wave function must be calculated from basic quantum theory. Therefore, the EFG tensor components are calculated as the expectation values of the corresponding one-electron operator (eq 6) via a wave function obtained from a self-consistent field or ab initio calculation.[20–29]

TABLE 1: Monomers and Dimers of Aluminum Chlorides

molecule	absolute energies, au, level	
	RHF/6-31G*	MP2/6-31G*
$AlCl_3$	−1620.57608635	−1621.00800956
$AlCl_4^-$	−2080.23047167	−2080.79637013
$EtAlCl_2$	−1239.67287050	−1240.24077086
$EtAlCl_3^-$	−1699.30831618	−1700.01149357
$Al_2Cl_7^-$	−3700.84744977	−3701.85481169
$Et_2Al_2Cl_5^-$	−2939.01933258	−2940.30084870
Al_2Cl_6	−3241.18122727	−3242.06125550
$Et_2Al_2Cl_4$	−2479.37497036	−2480.52747690

Quadrupole Moment. The quadrupole energy tensor matrix elements are proportional to the product of the scalar quadrupole moment Q and the gradient of the electric field $\mathbf{V}_{ij}$ in the following manner:

$$Q_{ij} = [eQ\mathbf{V}_{ij}/2I(2I - 1)] \tag{7}$$

The scalar quadrupole moment Q is defined as

$$eQ = \int \rho(r)(3z^2 - r^2)\,\mathrm{d}\tau = \int \rho(r)r^2(3\cos^2\theta - 1)\,\mathrm{d}\tau \tag{8}$$

where the integration is carried out over the nuclear charge density $\rho(r)$, and θ is the angle that the radius vector $\mathbf{r}$ makes with the internuclear axis.

The scalar quadrupole moment is a measure of the deviation of the nuclear charge density from spherical symmetry. It can exist only for $I > {}^1/_2$. The quadrupole tensor matrix elements are

$$\mathbf{Q}_{ij} = A[\mathbf{V}_{ij}/\mathbf{V}_{zz}] \tag{9}$$

where $A = e^2qQ/[2I(2I - 1)]$.

The field gradient tensor in a crystallographic coordinate system may be specified completely in terms of the parameters q and η and the three Eulerian angles, which describe the relative orientations of the crystallographic and principal coordinate systems. An alternative method of specifying the orientation of the principal axes entails the use of a directional cosine matrix.

Results and Discussion

Energies of Aluminum Chlorides. The structures of $AlCl_4^-$ (T_d), $AlCl_3$ (D_{3h}), and Al_2Cl_6 (D_{2h}) at the MP2/6-31G* level have been reported previously.[30–32] In addition to the ethyl chloride structures reported herein, we have extended the series of aluminum chloride structures to include $Al_2Cl_7^-$ at the MP2/6-31G* level. For purposes of comparison, the structures of $AlCl_4^-$, $AlCl_3$, and Al_2Cl_6 have also been determined at both the RHF/6-31G* and MP2/6-31G* levels. Table 1 contains the energies of all relevant structures as a convenience for the reader.

Structure of $Al_2Cl_7^-$. Figure 1 contains the resulting bent bridge structure of $Al_2Cl_7^-$ that belongs to the C_{2v} point group, as predicted by Gale and Osteryoung.[33] The Cl's in Figure 1 are in a staggered configuration, similar to those found in the crystal structure of $Te_4(Al_2Cl_7)_2$,[34] rather than the eclipsed structure reported for $Al_2Cl_7^-$ in $Pd_2(C_6H_5)_2(Al_2Cl_7)_2$.[35] The calculated Al(3)−Cl(1)−Al(2) bridging bond angle is 123.2°, significantly larger than values of 110.8 and 115.6° reported for the crystal structures of $Al_2Cl_7^-$.[34,35] The bond angles (deg) in Figure 1 are similar to those found in the solid state, such as Cl(4)−Al(2)−Cl(5) = 113.6° compared with 113.7 and 115.3°.[34,35] Additional comparison of bond angles (deg) include

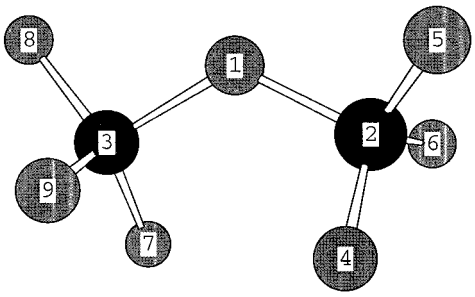

Figure 1. $Al_2Cl_7^-$ structure at the RHF/6-31G* level.

Cl(5)−Al(2)−Cl(6) = 112.7 vs 111.3 and 113.5, Cl(4)−Al(2)−Cl(6) = 114.5 vs 114.3 and 116.3, Cl(7)−Al(3)−Cl(1) = 107.0 vs 108.2 and 110.9.[34,35] Other bond angles (deg) are Cl(1)−Al(3)−Cl(9) = 105.9, Cl(1)−Al(3)−Cl(9) = 107.0, Cl(1)−Al(3)−Cl(9) = 101.9, Cl(1)−Al(2)−Cl(4) = 107.0, Cl(1)−Al(2)−Cl(5) = 101.8, Cl(1)−Al(2)−Cl(6) = 106.0, Cl(7)−Al(3)−Cl(8) = 113.6, Cl(9)−Al(3)−Cl(7) = 114.4, and Cl(9)−Al(3)−Cl(8) = 112.7.

The calculated bond lengths (Å) are Al(3)−Cl(1) = Al(2)−Cl(1) = 2.324, Al(3)−Cl(8) = Al(2)−Cl(5) = 2.137, Al(3)−Cl(7) = Al(2)−Cl(4) = 2.125, and Al(3)−Cl(9) = Al(2)−Cl(6) = 2.130. The Al−Cl bridge bond length of 2.324 Å is longer than average Al−Cl bridging bond lengths of 2.242[34] and 2.262 Å[35] found in the solid-state structures of $Al_2Cl_7^-$. The Al−Cl bond lengths in the $-AlCl_3$ groups found in the crystal structures are 2.102[34] and 2.099 Å,[35] compared with an average calculated value of 2.131 Å (Figure 1). The differences in Al−Cl−Al bond angles and bond lengths may be accounted for by crystal packing forces.

Vibrational Spectra and Spectral Assignments. Table 2 contains the calculated and experimental vibrational spectra for $AlCl_3$, Al_2Cl_6, $AlCl_4^-$, and $Al_2Cl_7^-$. In addition to the correlation between calculated and experimental frequencies, there is a qualitative match between calculated and experimental intensities. The vapor phase spectra of $AlCl_3$ and Al_2Cl_6 were taken from the work of Tomita et al.[36] The infrared and Raman spectra of the chloroaluminates has been the subject of numerous investigations.[3,33,37−39] The Raman and infrared experimental spectra were taken from the Raman studies of Rytter et al.[38] and the emission IR studies of Hvistendahl et al.[39]

As observed previously,[30] the calculated vibrational spectra of aluminum-containing compounds are remarkably close to the experimental values. This is apparent in a plot (Figure 2) of calculated vs experimental frequencies in which a scale factor of 0.97 accurately reproduces the experimental values with a correlation coefficient of 0.999. This may be compared with a typical scale factor of 0.89 used to reproduce vibrational energies for a wide range of molecules.[40,41] The inclusion of aluminum has a considerable effect on the correlation energy of these and similar compounds, as is indicated in the following sections on the dimer of ethylaluminum dichloride and its related anions.

Structures of the $EtAlCl_2$ Dimer, $EtAlCl_3^-$, and $Et_2Al_2Cl_5^-$. The existence of ethylaluminum dichloride as a trans dimer (C_{2v}) has previously been established by Weidlein in a Raman and IR study of alkylaluminum dichlorides, alkylaluminum dibromides, and alkylgallium dichlorides.[42] Figures 3−5 contain the structures of $EtAlCl_3^-$, $Et_2Al_2Cl_5^-$, and the trans dimer of ethylaluminum dichloride, all calculated at the RHF/6-31G* level.

TABLE 2: Vibrational Assignments for $AlCl_3$, Al_2Cl_6, $AlCl_4^-$, and $Al_2Cl_7^-$ (cm^{-1})[a]

assignt[b]	ν	I_{int}[c]	IR, Raman	Raman ν_{exp}	IR ν_{exp}	assignt[b]	ν	I_{int}[c]	IR, Raman	Raman ν_{exp}	IR ν_{exp}
					$AlCl_3$						
18	157	0.05	IR, R(m)dp	148dp(m)	151(w)	18	400	0	R(s)p	376p(s)	
18	213	0.26	IR		214(w)	18	642	1	IR., R(w)dp	610dp(w)	616(s)
					Al_2Cl_6						
1,18	23	0.002	IR			2,18	232	0	R(m)p	219p(s)	
18	68	0				18	268	0	R(w)dp	281dp(w)	
2,18	102	0	R(m)p	98p(s)		2,18	330	0.234	IR		320(m)
1,18	125.6	0	R(m)dp	112dp(m)		2,18	351	0	R(s)p	342p(s)	
18	125.7	0	R(m)dp	112dp(m)		18	431	0.498	IR		418(m)
2,18	138	0.036	IR		123(w)	2,18	497	1	IR		483(s)
2,18	150	0.057	IR		143(m)	2,18	537	0	R(m)p	511p(m)	
1,18	178	0	R(m)dp	168dp(m)		1,18	635	0	R(m)dp	614dp(m)	
1,2,18	190	0.028	IR		178(w)	1,18	646	0.932	IR		626(s)
					$AlCl_4^-$						
18; 1	121	0	R(m)dp	119dp(m)		18	353	0	R(m)p	346p(s)	
18	188	0.048	IR, R(m)dp	182dp(m)	183(m)	18; 1	511	1	IR, R(w)dp	488dp(w)	475(s)
					$Al_2Cl_7^-$						
1, 18	16	<0.001	R(vw)dp			4,18	196	0.182	IR, R(m)dp		179(m)
18	18	<0.001	R(vw)dp			4,18	207	0.001	IR, R(w)p		
18	40	<0.001	R(vw)dp			2,4,18	311	0.043	IR, R(m)p	312(s)p	308(w)
18	90	<0.001	R(m)dp			18; 1	332	0.617	IR, R(vw)dp		331(m)
18	91	<0.001	R(m)dp			18; 1	393	0.514	IR, R(w)dp		381(m)
2, 18	98	<0.001	R(m)p	99(m)p		18	442	0.065	IR, R(m)p	432(w)p	439(w)
1,3,18	125	0.003	IR, R(w)dp			18	553	0.343	IR, R(w)dp		525(s)
1,3,18	151	0.026	IR, R(w)p			18	558	0.186	IR, R(m)dp		
1,3,18	163	0.015	IR, R(m)dp		158(w)	18; 1	572	1	IR, R(w)dp		
1,18	168	<0.001	R(m)dp	164(m)dp		18; 1,3	573	0.868	IR, R(w)p		
18	183	0.05	IR, R(m)dp								

[a] Assignments of vibrational frequencies: (1) Cl−Al−Cl asymmetric bend; (2) Cl−Al−Cl symmetric bend; (3) Al−Cl−Al asymmetric bend; (4) Al−Cl−Al symmetric bend; (5) methylene asymmetric bend; (6) methylene symmetric bend; (7) methyl asymmetric bend; (8) methyl symmetric bend; (9) C−C−H bend; (10) Al−C−C bend; (11) asymmetric methylene asymmetric stretch; (12) symmetric methylene H−C−H stretch; (13) asymmetric methyl H−C−H stretch; (14) methyl symmetric H−C−H stretch; (15) methylene deform.; (16) methyl symmetric deform.; (17) methyl asymmetric deform.; (18) Al−Cl streetch; (19) Al−C stretch. [b] Major assignments; minor assignments. [c] Intensity normalized to the most intense line = 1.00.

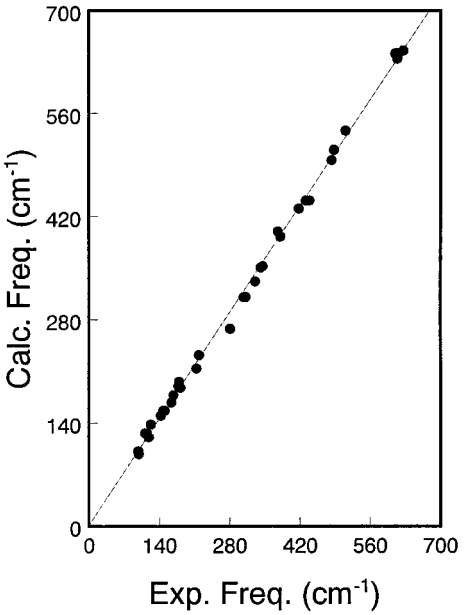

Figure 2. Correlation diagram for the vibrational spectrum of $AlCl_3$, Al_2Cl_6, $AlCl_4^-$, and $Al_2Cl_7^-$: computed vs measured IR and Raman transitions. Scale factor = 0.97 and correlation coefficient = 0.999.

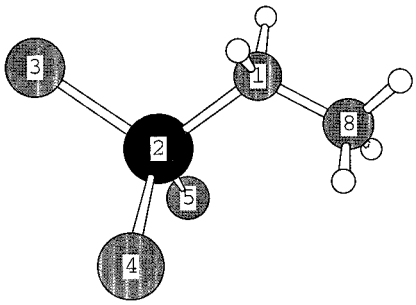

Figure 3. $EtAlCl_3^-$ structure at the RHF/6-31G* level.

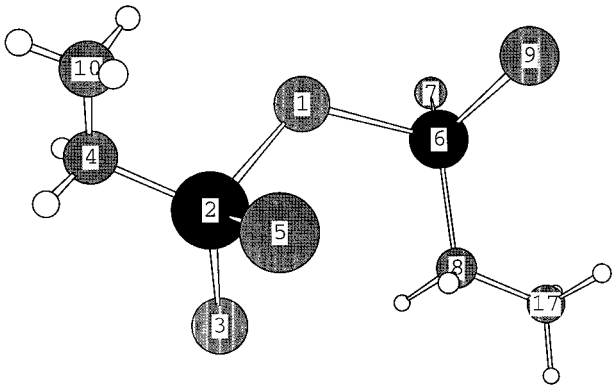

Figure 4. *trans*-$Et_2Al_2Cl_5^-$ structure at the RHF/6-31G* level.

Ethylaluminum Trichloride. $EtAlCl_3^-$ (Figure 3) is similar to $AlCl_4^-$, in that the Al−(Cl$_3$)−C(1) group occupies a slightly deformed tetrahedron. Bond angles (deg): C(1)−Al−Cl(4) = 111.2, C(1)−Al−Cl(5) = 111.2, C(1)−Al−Cl(3) = 109.9, Cl(4)−Al−Cl(3) = 108.2, Cl(4)−Al−Cl(5) = 108.0, C(8)−C(1)−Al = 116.4. The bond lengths are (Å): Al−C(1) = 1.989, C(1)−C(8) = 1.537, Al−Cl(4) = 2.201, Al−Cl(3) = 2.200, Al−Cl(5) = 2.201.

Ethylaluminum Pentachloride. The calculated structure of trans $Et_2Al_2Cl_5^-$ (Figure 4) is similar to the structure of the heptachloroaluminate ion shown in Figure 2. Bond angles (deg): C(10)−C(4)−Al(2) = 115.2, C(17)−C(8)−Al(6) = 114.5, Cl(7)−Al(6)−C(8) = 116.0, Cl(9)−Al(6)−C(8) = 115.9, Cl(3)−Al(2)−C(4) = 115.2, Cl(5)−Al(2)−C(4) = 115.2, Cl(9)−Al(6)−Cl(7) = 110.0, Cl(1)−Al(6)−C(8) = 107.7, Cl(1)−Al(6)−Cl(7) = 102.7, Cl(1)−Al(6)−Cl(9) = 102.7, Cl(5)−Al(2)−Cl(3) = 111.1, Cl(1)−Al(2)−C(4) = 102.3, Cl(1)−Al(2)−Cl(3) = 105.8, Cl(1)−Al(2)−Cl(5) = 105.8, Al(2)−Cl(1)−Al(6) = 124.2. Bond lengths (Å): C(4)−C(10) = 1.538, C(8)−C(17) = 1.539, Al(6)−C(8) = 1.969, Al(6)−Cl(7) = 2.164, Al(6)−Cl(9) = 2.165, Al(2)−C(4) = 1.974, Al(2)−Cl(3) = 2.161, Al(2)−Cl(5) = 2.161, Al(6)−Cl(1) = 2.363, Al(2)−Cl(1) = 2.340.

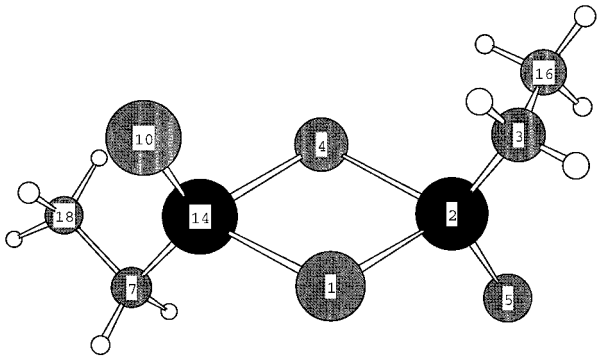

Figure 5. *trans*-$(EtAlCl_2)_2$ structure at the RHF/6-31G* level.

Ethylaluminum Dichloride Trans Dimer. Figure 5 contains the calculated structure of *trans*-$(EtAlCl_2)_2$. There is a small deviation from C_{2v} symmetry as the ethyl groups are slightly out of their initial plane of symmetry. Bond angles (deg): Al(14)−C(7)−C(18) = Al(2)−C(3)−C(16) = 115.1, C(7)−Al(14)−Cl(10) = 123.8, Cl(1)−Al(14)−Cl(10) = 107.8, Cl(1)−Al(14)−C(7) = 111.4, Cl(4)−Al(14)−Cl(10) = Cl(4)−Al(2)−Cl(5) = 107.6, Cl(4)−Al(14)−C(7) = Cl(4)−Al(2)−C(3) = 111.9, Cl(4)−Al(14)−Cl(1) = Cl(4)−Al(2)−Cl(1) = 88.6, Al(2)−Al(14)−Cl(10) = 115.1, Al(2)−Al(14)−C(7) = 121.0, Al(2)−Al(14)−Cl(1) = Al(2)−Al(14)−Cl(4) = Cl(1)−Al(2)−Al(14) = Cl(4)−Al(2)−Al(14) = 44.3, Al(2)−Cl(1)−Al(14) = 91.5, Al(2)−Cl(4)−Al(14) = 91.4, C(3)−Al(2)−Cl(5) = 123.9, Al(14)−Al(2)−Cl(5) = 115.2, Al(14)−Al(2)−C(3) = 120.9, Cl(1)−Al(2)−Cl(5) = 107.8, Cl(1)−Al(2)−C(3) = 111.4. Bond lengths (Å): C(7)−C(18) = 1.540, C(3)−C(16) = 1.541, Al(14)−Cl(10) = Al(2)−Cl(5) = 2.112, Al(14)−C(7) = 1.954, Al(2)−C(3) = 1.953, Cl(1)−Al(14) = Al(2)−Cl(1) = 2.318, Cl(4)−Al(14) = 2.319, Al(2)−Cl(4) = 2.320, Al(2)−Al(14) = 3.320.

Vibrational Spectra and Spectral Assignments. Table 3 contains the calculated and experimental vibrational spectra for dimeric *trans*-$EtAlCl_2$, $EtAlCl_3^-$, and $Et_2Al_2Cl_5^-$. Weidlein's Raman and IR spectra[42] provide a good correlation between calculated and experimental energies, and there is a qualitative match between calculated and experimental intensities. Other workers report Raman spectra of $EtAlCl_2$, $EtAlCl_3^-$, and $Et_2Al_2Cl_5^-$, using combinations of ethylaluminum dichloride and 1-butyl-3-methylimidazolium chloride to produce $EtAlCl_3^-$ and $Et_2Al_2Cl_5^-$.[10] The Raman spectrum of ethylaluminum dichloride[10] is similar to that reported by Weidlein,[42] as shown in Table 3. In addition, the Raman bands at 150, 182, 273, 367, and 621 cm^{-1} attributed to $EtAlCl_3^-$ match well with the calculated spectra in Table 3. Of these Raman bands, only the 273 cm^{-1} band matches a similar Raman band for neat ethylaluminum dichloride. Only 5 of the 14 Raman bands[12] assigned to $Et_2Al_2Cl_5^-$ match well with the calculated values (166, 178, 253, 398, and 420 cm^{-1}) included in Table 3. The other Raman bands attributed to $Et_2Al_2Cl_5^-$ fail to match either polarization or energy assignments such as the intense, polarized

TABLE 3: Vibrational Assignments for $(EtAlCl_2)_2$, $EtAlCl_3^-$, and $Et_2Al_2Cl_7^-$ (cm^{-1})[a]

$EtAlCl_2$ Dimer

assignt	ν	I_{rel}	IR, Raman	IR ν_{exp}	Raman ν_{exp}	assignt	ν	I_{rel}	IR, Raman	IR ν_{exp}	Raman ν_{exp}
5,7; 1,3,9,18,19	18	0.003	IR R(vw)dp			5; 7	704	0.086	IR, R(m)p		657p(m−s)
7; 5,9	33	<0.001	R(w)dp			5; 8,10,19	705	0.669	IR R(vw)p	663(s)	
6,8,9	42	0.002	IR R(vw)dp			5,7	1024	0.084	IR, R(w)p		
5,7	60	0.001	IR, R(w)dp			6,8	1025	0.019	IR, R(w)p		
7; 4,9,18	92	0.007	IR R(w)dp			5,7	1039.2	0.002	IR, R(m)p		
6,9; 1,4,18	98	0.007	IR, R(w)dp			5; 7	704	0.086	IR, R(m)p		
6,8; 1,3,9,18	115	0.014	IR, R(w)p			5,7; 10	1039.4	0.002	IR, R(m)p		
5,7; 2,4,18	125	0.001	IR, R(m)dp			6,8; 10,19	1091	0.174	IR, R(m)dp		
5,7	130	0.025	IR, R(w)dp	∼130(m)		6,8; 10,19	1094	0.079	IR, R(m)p		
5,7; 2,4,18	149	0.005	IR, R(m)dp			15; 8	1376	0.005	IR, R(w)dp		
5,7; 2,4	185	0.001	IR, R(m)p			15,7	1377	0.006	IR, R(m)p		
1,3,5,7,18	186	0.066	IR R(vw)dp	172(m)		15,7	1378.8, 1378.9	0.007, 0.010	IR, R(m)p		
2,4,7,18,19	242	<0.001	R(w)dp		213dp(w)	16; 6	1564.9	0.029	IR, R(m)dp		
7; 5	247	0.001	IR R(w)p			16; 5	1565.2	<0.001	IR, R(m)p		
7;5	253	0.003	IR R(vw)dp			5; 17	1594.2	0.019	IR, R(s)dp		
7; 2,4,5,10,19	272	0.066	IR, R(w)dp	268(m)		5; 17	1594.3	0.007	IR, R(s)p		
5,7; 2,4,10	288	0.007	IR R(m)p		274p(m)	17	1646.2, 1646.3	0.006, 0.010	IR, R(s)dp		
6,8; 1,3,18	351	0.087	IR, R(m)p		346p(vs)	17	1655.2, 1655.3	0.027, 0.014	IR, R(s)dp		
6,8; 1,3,10,18	353	0.794	IR R(vw)p	323(s)		12	3173.2, 3173.5	0.065, 0.070	IR, R(vs)p		
2,4,18,19; 5,7,10	426	0.674	IR R(vw)p	396(s)		13	3196	0.174	IR, R(m)p		
2,4,5,7,10,18,19	496	1	IR R(vw)dp	486(s)		13	3197	0.15	IR, R(vs)dp		
2,4,5,7,18; 10,19	515	<0.001	R(s)p		502p(s)	11	3207.7, 3208.2	0.036, 0.037	IR, R(vs)dp		
5,7; 2,4,10	674	0.437	IR R(vw)p			14	3253.7, 3254.0	0.237, 0.148	IR, R(vs)p		
5; 2,4,7,10	677	0.051	IR, R(s)p			13	3259.9, 3260.3	0.132, 0.204	IR, R(vs)dp		

$EtAlCl_3^-$

assignt	ν	I_{ini}	IR, Raman	Raman ν_{exp}	assignt	ν	I_{ini}	IR, Raman	Raman ν_{exp}
6,8	54	<0.001	R(w)dp		5,7; 10	1033	0.008	IR, R(s)p	
5,7,18	95	0.001	IR,R(w)dp		6,7; 10	1093	0.134	IR, R(m)p	
6,8,19; 10	120	<0.001	R(w)dp		15; 10,17	1367	0.019	IR, R(w)p	
10,18	147	0.017	IR,R(m)dp		15; 16	1380	0.014	IR, R(m)dp	
6,8	162	0.02	IR,R(m)dp	150dp	15; 17	1553	0.016	IR, R(m)dp	
10,18	188	0.065	IR,R(m)dp	182dp	15; 17	1602	0.016	IR, R(s)dp	
6,8	260	0.003	IR,R(w)dp		15; 17	1651	0.008	IR, R(s)dp	
10,18;6,8	288	0.001	IR, R(m)p	273dp	16	1655	0.004	IR, R(vs)dp	
5,7,10,18	376	0.139	IR, R(m)p	367p	11,13	3139	0.322	IR, R(vs)dp	
6,19; 8,10	465	0.75	IR,R(m)dp		11,13	3158	0.464	IR, R(vs)p	
10,19; 5,7	487	1	IR, R(w)dp		12; 14	3170	0.213	IR, R(vs)dp	
5,10,18; 7	630	0.494	IR, R(m)p	621dp	12; 14	3213	0.298	IR, R(vs)p	
6,8; 10	690	0.347	IR, R(w)dp		12; 14	3243	0.335	IR, R(s)dp	
6; 8	1010	0.056	IR, R(m)dp						

$Et_2Al_2Cl_5^-$

assignt	ν	I_{int}	IR, Raman	Raman ν_{exp}	assignt	ν	I_{int}	IR, Raman	Raman ν_{exp}
1,3,18; 5,7,10,19	5	0.001	IR R(vw)dp		2,6,8,10,18,19	652	0.154	IR, R(m)p	
7; 1,3,5,10,18	20	0.002	IR R(vw)dp		2,8,10,19; 6,18	663	0.4	IR, R(m)p	
8; 2,6,10	40	0.001	IR, R(w)p		5,7; 19	699	0.032	IR, R(w)dp	
5,7; 1	47	<0.001	IR, R(w)dp		5,7	701	0.381	IR, R(w)dp	696dp(w)
5,7; 1	49	<0.001	IR, R(w)dp		5,7	1018	0.027	IR, R(m)dp	
5,7; 1,3,10	77	<0.001	IR, R(w)dp		5,7	1024	0.04	IR, R(w)dp	
8; 2,4,6,10	82	0.003	IR, R(w)dp		6,8; 19	1037	0.002	IR, R(m)p	
5; 1,3,7,18	93	<0.001	R(m)dp		6,8,10; 19	1039	0.002	IR, R(m)p	
5; 1,3,7,10	123	0.001	IR, R(w)dp		6,8; 19	1088	0.149	IR, R(m)dp	
8; 2,4,6,18	124	0.031	IR, R(w)p		6,8,10	1091	0.039	IR, R(m)p	
5,7; 1,3	145.7	<0.001	IR, R(m)dp		6,8,10; 19	1373, 1377	0.012, 0.012	IR, R(m)p	
6,8; 2,4,18	145.9	0.039	IR, R(w)p		5,7; 19	1381, 1384	0.005, 0.007	IR, R(m)dp	
7; 2,3,5,10,18	160	0.015	IR, R(w)dp		16	1556	0.013	IR, R(m)p	
2,4,6,8,10,18	166	0.003	IR, R(m)dp	166dp(m)	16	1557	0.009	IR, R(m)p	
2; 4,6,8,10	179	0.012	IR, R(m)p	178dp(m)	15	1601, 1602	0.007, 0.014	IR, R(m)p	
2,8; 4,6	238	0.034	IR, R(m)p		17	1649, 1650	0.004, 0.004	IR, R(m)p	
7; 5	258	0.001	IR, R(w)dp	253p(m)	17	1656.1, 1656.5	0.006, 0.006	IR, R(m)dp	
7; 5,19	259	0.003	IR R(vw)dp		12,14	3160, 3172	0.130, 0.245	IR, R(s)p	
4,6,8,18; 10,19	287	0.047	IR, R(w)p		12,14	3175, 3182	0.182, 0.050	IR, R(vs)p	
3,6,10,18,19	339	1	IR, R(w)dp		11	3191	0.064	IR, R(vs)dp	
2,6,10,18	376	0.058	IR, R(m)p		11,13	3210	0.011	IR, R(vs)dp	
2,4,6,8,10,18	406	0.23	IR, R(w)p	398p(m)	14	3222	0.156	IR, R(vs)dp	
2,4,6,18,19	433	0.099	IR, R(m)p	420p(s)	14	3223	0.212	IR, R(vs)dp	
3,5,19; 7,18	505	0.112	IR, R(m)dp		13	3244, 3246	0.171, 0.201	IR, R(vs)dp	
1,5,18; 7,19	513	0.65	IR, R(w)dp						

[a] Assignments of vibrational frequencies: (1) Cl−Al−Cl asymmetric bend; (2) Cl−Al−Cl symmetric bend; (3) Al−Cl−Al asymmetric bend; (4) Al−Cl−Al symmetric bend; (5) methylene asymmetric bend; (6) methylene symmetric bend; (7) methyl asymmetric bend; (8) methyl symmetric bend; (9) C−C−H bend; (10) Al−C−C bend; (11) asymmetric methylene asymmetric stretch; (12) symmetric methylene H−C−H stretch; (13) asymmetric methyl H−C−H stretch; (14) methyl symmetric H−C−H stretch; (15) methylene deform.; (16) methyl symmetric deform.; (17) methyl asymmetric deform.; (18) Al−Cl streetch; (19) Al−C stretch.

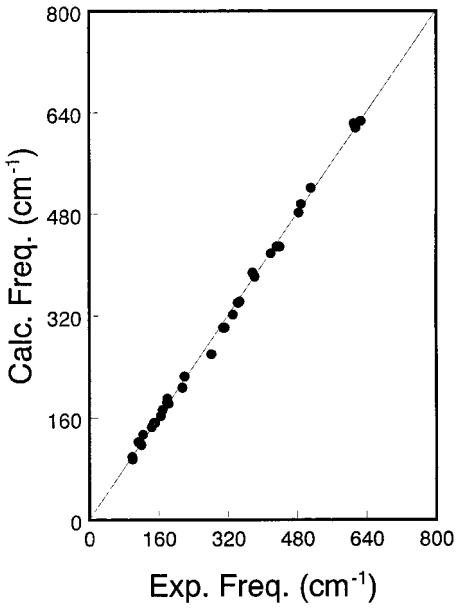

Figure 6. Correlation diagram for the vibrational spectrum of $EtAlCl_3^-$, $Et_2Al_2Cl_5^-$, and $(EtAlCl_2)_2$: computed vs measured IR and Raman transitions. Scale factor = 0.97 and correlation coefficient = 0.999.

band at 349 cm^{-1} which is also observed in the Raman spectrum of $EtAlCl_4^-$.[10]

Figure 6 is a plot of calculated vs experimental frequencies in which a scale factor of 0.97 accurately reproduces the experimental values with a correlation coefficient of 0.999, in a manner identical to the results in Figure 2 for aluminum chloride and related chloroaluminates. It is apparent that the vibrational spectra of this type of aluminum containing compounds can be accurately reproduced using ab initio methods at the 6-31G* level.

^{27}Al Quadrupole Coupling Constant and EFG Calculations. Although ^{27}Al has a natural abundance of 100%, there are a limited number of experimental NQR results that are usefulfor comparison with ab initio calculations. In this study four molecules (AlF and the dimers of $AlCl_3$, $AlBr_3$, and $Al(CH_3)_3$)[43−46] that provided 12 points are used in the curve-fitting process. The data and results of the various levels of computation for these molecules are contained in Table 4. It should be noted that the experimental NQCC of Al_2Br_6 was changed from 13.86 MHz to −13.86 MHz.[43] The EFG ($\mathbf{V}_{ij}$) eigenvalues of the three tensor components ($\mathbf{V}_{xx}$, $\mathbf{V}_{yy}$, and $\mathbf{V}_{zz}$) were calculated for these molecules at the ab initio levels HF/3-21G, B3LYP/6-31G*//HF/3-21G, HF/6-31G*//HF/3-21G, HF/6-31G*, B3LYP/6-31G*//HF/6-31G*, B3LYP/6-31G*, and B3LYP/cc-pVTZ. The experimental χ_{ij}'s were plotted against the computed values of $\mathbf{V}_{ij}$ for each basis set, and the linear regression results of each plot are contained in Table 4. The literature values of Q range from −140 to −150 mb with the suggested value of 140.3 mb.[27]

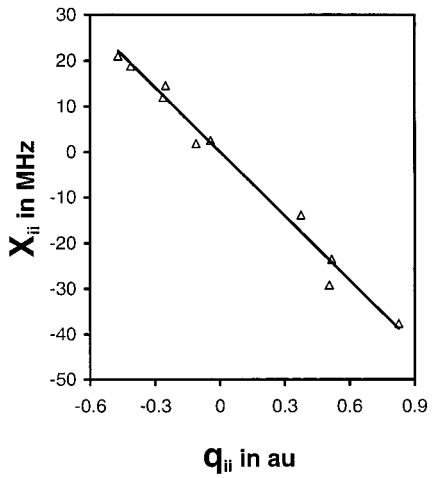

Figure 7. Experimental NQCC's (χ_{ij}) vs theoretical EFG's (q_{ij}) at the HF/3-21G level.

As mentioned previously, the sign for the value of χ_{zz} for Al_2Br_6 had to be changed for the fits to be linear. When Casbella et al.[43] reported the value of the $AlBr_3$ NQCC, they suggested the possible existence of a dimer with a NQCC value of 13.86 MHz and an asymmetry parameter of 0.73. Our calculations show that the $\mathbf{V}_{zz}$ component for all computational levels to be positive, which results in a negative NQCC with the B3LYP/cc-PVTZ calculation, yielding an asymmetry parameter of 0.71 that is very close to the one reported by Casbella and co-workers.[43] The calculation of the $AlBr_3$ monomer yielded an asymmetry parameter of 0.0 for all computational levels and a theoretical estimate of approximately 25 MHz for the ^{27}Al NQCC, supporting the existence of the dimer with its negative NQCC.

Although only four molecules were used in the fit at all computational levels, the fit at the higher computational levels produced deviations smaller than one might expect.[27] The HF/3-21G calculation yielded the highest value of 199.69 mb for Q with an R^2 correlation of 0.9843 (Figure 7) that is the worst when compared to the rest of the linear regression fits. The optimized geometry at the HF/3-21G was used for single point calculations at the HF/6-31G* and B3LYP/6-31G* levels. These

TABLE 4: Experimental and Theoretical EFG's and NQCC's for ^{27}A

cmpd	exp	HF/3-21G	B3LYP/6-31G*// HF/3-21G	HF/6-31G*// HF3-21G	HF/6-31G*	B3LYP/6-31G*// HF/6-31G*	B3LYP/6-31G*	B3LYP/cc-pVTZ
AlF	−37.6	0.826122	0.934487	0.960906	0.980233	0.952111	0.92232	1.12818
	18.8	−0.413061	−0.467243	−0.480453	−0.49012	−0.476055	−0.4612	−0.5641
	18.8	−0.413061	−0.467243	−0.480453	−0.49012	−0.476055	−0.4612	−0.5641
Al_2Cl_3	−29.2	0.504777	0.60947	0.64632	0.756157	0.703079	0.69111	0.9465
	14.6	−0.252389	−0.304735	−0.32316	−0.37808	−0.35154	−0.3456	−0.4733
	14.6	−0.252389	−0.304735	−0.32316	−0.37808	−0.35154	−0.3456	−0.4733
Al_2Br_6	−13.86	0.374415	0.319279	0.384182	0.396449	0.337676	0.33585	0.41337
	11.9889	−0.264217	−0.260004	−0.324181	−0.32302	−0.265094	−0.2602	−0.3536
	1.8711	−0.110198	−0.059276	−0.060001	−0.07342	−0.072581	−0.0757	−0.0597
$Al_2(CH_3)_6$	−23.546	0.516186	0.619568	0.691034	0.67855	0.610918	0.6144	0.75581
	21.003	−0.472453	−0.518034	−0.579368	−0.57995	−0.519561	−0.5212	−0.6663
	2.543	−0.043733	−0.101534	−0.111666	−0.0986	−0.091357	−0.0932	−0.0895
Slope(MHz)		−46.92	−41.729	−38.968	−37.457	−40.11	−40.845	−32.167
R^2		0.9843	0.9927	0.9909	0.998	0.9985	0.9981	0.9986
$-Q$(mb)		199.69	177.6	165.85	159.42	170.71	173.83	136.9

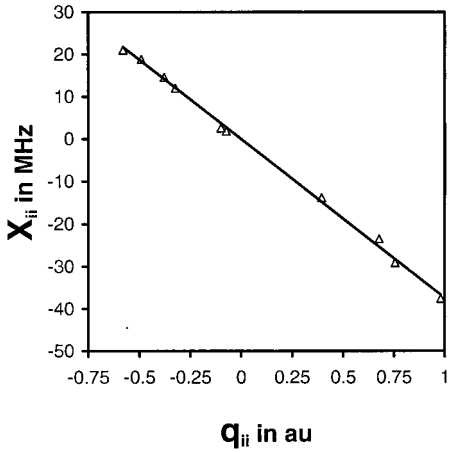

Figure 8. Experimental NQCC's (χ_{ij}) vs theoretical EFG's (q_{ij}) at the HF/6-31G* level.

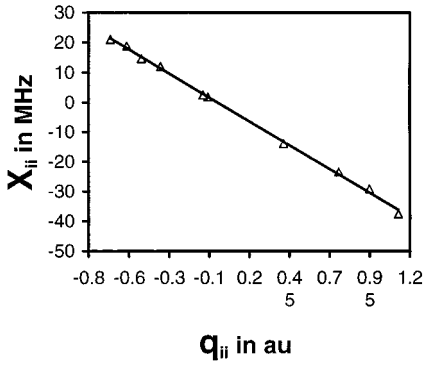

Figure 9. Experimental NQCC's (χ_{ij}) vs theoretical EFG's (q_{ij}) at the DFT B3LYP/cc-pVTZ level.

single point calculations improved the fit and lowered the value of Q to 165.85 and 177.60 mb, respectively, with an R^2 correlation of 0.991 and 0.993 (Table 4). The fully optimized geometry at the HF/6-31G* level (Figure 8) lowered Q to 159.42 mb with an R^2 correlation of 0.998, bringing it closer to the literature values.[27] The single point calculation at the B3LYP/6-31G* level using the fully optimized geometry at HF/6-31G* level produced a Q value of 170.71 mb with an R^2 correlation of 0.9985, a slightly better fit than the HF/6-31G* result. The fully optimized geometry at the B3LYP/6-31G* level produced a Q of 173.83 mb with an R^2 correlation of 0.9981 suggesting that the geometry obtained at a lower level might result in to a better fit by doing a single point calculation at a higher basis set. Finally, the best fit obtained was the B3LYP/cc-pVTZ calculation, which gave a Q of 136.90 mb (R^2 correlation of 0.9986), which is close to the suggested value of 140.3 mb.[27]

Conclusions

The vibrational spectra of $AlCl_3$, Al_2Cl_6, $AlCl_4^-$, $EtAlCl_3^-$, $Al_2Cl_7^-$, $Et_2Al_2Cl_5^-$, and *trans*-$Et_2Al_2Cl_4$ calculated at the RHF/6-31G* level are in good agreement with the experimental infrared and Raman spectra. The presence of Al lowers the scale factor to 0.97 and yields a correlation factor of 0.999 for the vibrational frequency correlation. The effect of Al on the vibrational calculations has been previously noted by other investigators[32] and appears to be a general trend for this element in ab initio calculations.

Finally, the ^{27}Al quadrupole coupling constants and asymmetry parameters of the electric field gradient tensor have been calculated for Al_2Br_6, Al_2Cl_6, AlF, and $Al_2(CH_3)_6$ at the HF/3-21G, B3LYP/6-31G*//HF/3-21G, HF/6-31G*//HF/3-21G, HF/6-31G*, B3LYP/6-31G*//HF/6-31G*, B3LYP/6-31G*, and B3LYP/cc-pVTZ levels. Each level of calculation is correlated with experimental values of the ^{27}Al NQCC's. The correlation coefficient between experimental and theoretical ^{27}Al nuclear quadrupole coupling constants (NQCC) is lowest (0.984) for the HF/3-21G calculation and highest (0.9986) for the highest level of theory, B3LYP/cc-pVTZ. The theoretical values of the ^{27}Al NQCC vary from −199.69 mb (HF/3-21G) to −136.9 mb (B3LYP/cc-pVTZ) and may be compared with a suggested value[27] of −140.3 mb.

Acknowledgment. G.J.M. thanks the OSU computer center for their generous donation of computer time. W.R.C. thanks the Deutsche Forschungsgemeinschaft for a Mercator Visiting Professorship and Professor W. Stahl at RWTH for his advice and the use of his extensive library.

References and Notes

(1) Øye, H. A.; Rytter, E.; Klaeboe, P.; Cyvin, S. J. *Acta Chem. Scand.* **1971**, *25*, 559−576.
(2) Koch, V. R.; Miller, L. L.; Osteryoung, R. A. *J. Am. Chem. Soc.* **1976**, *98*, 5277−5284.
(3) Gale, R. J.; Gilbert, B.; Osteryoung, R. A. *Inorg. Chem.* **1978**, *17*, 2728−2729.
(4) Wilkes, J. S.; Levisky, J. A.; Wilson, R. A.; Hussey, C. L. *Inorg. Chem.* **1982**, *21*, 1263−1264.
(5) Zawodzinski, T. A.; Kurland, R.; Osteryoung, R. A. *J. Phys. Chem.* **1987**, *91*, 962−966.
(6) Gilbert, B.; Williams, S. D.; Mamantov, G. *Inorg. Chem.* **1988**, *27*, 2359−2363.
(7) Carper, W. R.; Pflug, J. L.; Elias, A. M.; Wilkes, J. S. *J. Phys. Chem.* **1992**, *96*, 3828−3833.
(8) Keller, C. E.; Carper, W. R. *J. Magn. Reson., Ser. A* **1994**, *110*, 125−129.
(9) Keller, C. E.; Carper, W. R. *Inorg. Chim. Acta* **1993,** *210*, 203−208.
(10) Gilbert, B.; Chauvin, Y.; Guibard, I. *Vibr. Spectrosc.* **1991**, *1*, 299−304.
(11) Keller, C. E.; Piersma, B. J.; Mains, G. J.; Carper, W. R. *Inorg. Chem.* **1994**, *33*, 5601−5603.
(12) Keller, C. E.; Piersma, B. J.; Carper, W. R. *J. Phys. Chem.* **1995**, *99*, 12998−13001.
(13) Carper, W. R.; Mains, G. J.; Piersma, B. J.; Manssfield, S. L.; Larive, C. K. *J. Phys. Chem.* **1996**, *100*, 4724−4728.
(14) Larive, C. K.; Lin, M.; Kinnear, B. S.; Piersma, B. J.; Keller, C. E.; Carper, W. R. *J. Phys. Chem.* **1998**, *102B*, 1717−1723.
(15) Frisch, M. J.; Trucks, G. W.; Head-Gordon, M.; Gill, P. M. W.; Wong, M. W.; Foresman, J. B.; Johnson, B. G.; Schlegel, H. B.; Robb, M. A.; Replogle, E. S.; Gomperts, R.; Andres, J. L.; Raghavachari, K.; Binkley, J. S.; Gonzalez, C.; Martin, J. L.; Fox, D. J.; Defrees, D. J.; Baker, J.; Stewart, J. J. P.; Pople, J. A. *Gaussian 92*, revision A.2; Gaussian, Inc.: Pittsburgh, PA, 1992.
(16) Frisch, M. J.; Trucks, G. W.; Schlegel, H. B.; Gill, P. M. W.; Johnson, B. G.; Robb, M. A.; Cheeseman, J. R.; Keith, T.; Petersson, G. A.; Montgomery, J. A.; Raghavachari, K.; Al-Laham, M. A.; Zakrzewski, V. G.; Ortiz, J. V.; Foresman, J. B.; Cioslowski, J.; Stefanov, B. B.; Nanayakkara, A.; Challcombe, M.; Peng, C. Y.; Ayala, P. Y.; Chen, W.; Wong, M. W.; Andres, J. L.; Replogle, E. S.; Gomperts, R.; Martin, R. L.; Fox, D. J.; Binkley, J. S.; Defrees, D. J.; Baker, J.; Stewart, J. J. P.; Head-Gordon, M.; Gonzalez, C.; Pople, J. A. *Gaussian 94*, revision C.3; Gaussian, Inc.: Pittsburgh, PA, 1995.
(17) Frisch, M. J.; Trucks, G. W.; Schlegel, H. B.; Gill, P. M. W.; Johnson, B. G.; Robb, M. A.; Cheeseman, J. R.; Keith, T.; Petersson, G. A.; Montgomery, J. A., Jr.; Raghavachari, K.; Al-Laham, M. A.; Zakrzewski, V. G.; Ortiz, J. V.; Foresman, J. B.; Cioslowski, J.; Stefanov, B. B.; Nannayakkara, A.; Challacombe, M.; Peng, C. Y.; Ayala, P. Y.; Chen, W.; Wong, M. W.; Andres, J. L.; Replogle, E. S.; Gomperts, R.: Martin, R. L.; Fox, D. J.; Binkley, J. S.; Defrees, D. J.; Baker, J.; Stewart, J. J. P.; Head-Gordon, M.; Gonzalez, C.; Pople, J. A. *Gaussian 98*, revision A.7; Gaussian, Inc.: Pittsburgh, PA, 1998.
(18) Stewart, J. J. P. MOPAC, *Quantum Chemistry Prog. Exch.* No. 455, 1983.
(19) Moeller, C.; Plesset, M. S. *Phys. Rev.* **1934**, *46*, 678.
(20) Kellog, J. M. B.; Rabi, I. I.; Ramsey, N. F.; Zacharias, J. R. *Phys. Rev.* **1940**, *57*, 677−695.
(21) Kern, C. W.; Karplus, M. *J. Chem. Phys.* **1964**, *42*, 1062−1071.

(22) Lucken, E. A. C. *Nuclear Quadrupole Coupling Constants*; Academic Press: London, 1969.
(23) Palmer, M. H. *Z. Naturforsh. A* **1986**, *41*, 147−162.
(24) Palmer, M. H. *Z. Naturforsch. A* **1990**, *45*, 357−367.
(25) Palmer, M. H. *Z. Naturforsch. A* **1992**, *47*, 203-216.
(26) Pound, R. V. *Phys. Rev.* **1950**, *79*, 685−702.
(27) Pyyko, P. *Z. Naturforsch*. A **1992**, *47*, 189−196.
(28) Schuler, H.; Schmidt, T. *Z. Phys*. **1935**, *94*, 457−462
(29) Townes, C. H.; Dailey, B. P. *J. Chem. Phys.* **1948**, *17*, 782−796.
(30) Mains, G. J.; Bock, C. W.; Trachman, M.; Mastryukov, V. S. *J. Mol. Struct*. (*THEOCHEM*) **1992**, *274*, 277−287.
(31) Boch, C. W.; Trachman, M.; Mains, G. J. *J. Phys. Chem*. **1993**, *97*, 2456−2554.
(32) Bock, C. W.; Trachtman, M.; Mains, G. J. *J. Phys. Chem*. **1994**, *98*, 478−485.
(33) Gale, R. J.; Osteryoung, R. A. *Inorg. Chem*. **1980**, *19*, 2240−2242.
(34) Couch, T. W.; Lokken, D. A.; Corbett, J. D. *Inorg. Chem*. **1972**, *11*, 357−362.
(35) Allegra, G.; Casogrande, G. T.; Immirzi, A.; Porri, L.; Vitulli, G. *J. Am. Chem. Soc*. **1970**, *92*, 289−293.
(36) Tomita, T.; Sjøgren, C. E.; Klaeboe, P.; Papatheodorou, G.; Rytter, E. *J. Raman Spectrosc.* **1983**, *14*, 415−425.
(37) Cyvin, S. J.; Klaeboe, P.; Rytter, E.; Øye, H. *J. Chem. Phys*. **1970**, *52*, 2776−2777.
(38) Rytter, E.; Øye, H.; Cyvin, S. J.; Cyvin, B. N.; Klaeboe, P. J. *Inorg. Nucl. Chem.* **1973**, *35*, 1185−1198.
(39) Hvistendahl, J.; Klaeboe, P.; Rytter, E.; Øye, H. A. *Inorg. Chem*. **1984**, *23*, 706−715.
(40) Hehre, W. J.; Radom, L.; Schleyer, P. von, R.; Pople, J. A. *Ab Initio Molecular Orbital Theory*; Wiley: New York, 1986.
(41) Carper, W. R.; Zandler, M.; Mains, G. J. *J. Phys. Chem*. **1993**, *97*, 9091−9095.
(42) Weidlein, J. *J. Organomet. Chem.* **1969**, *17*, 213−222.
(43) Casabella, P. A.; Bray, P. J.; Barnes, R. G. *J. Chem. Phys*. **1959**, *30*, 1393−1396.
(44) Casabella, P. A.; Miller, N. C. *J. Chem. Phys.* **1964**, *40*, 1363−1368.
(45) Lide, D. R., Jr. *J. Chem. Phys*. **1965**, *42*, 1013−1018.
(46) Dewar, M. J. S.; Patterson, D. B. *Chem. Commun*. **1970**, 544.